Identification of lead compounds against human hepatitis B viral capsid protein in three medicinal plants through *in silico* method

Subin Mathew M S[1], Sreekumar S[2], Biju C K[3]

[1,2,3]*Biotechnology & Bioinformatics Division, Saraswathy Thangavelu Centre, Jawaharlal Nehru Tropical Botanic Garden and Research Institute, Puthenthope, Thiruvananthapuram, PIN 695586, Kerala, India*
[2]*Corresponding author: drsreekumar@rediffmail.com*

Abstract: *Hepatitis B viral infection is a serious health problem in all over the world and its treatment is expensive with limited success (30-40%. The current treatment system may induce serious side effects. It is well acknowledged that plant-derived drug molecules are safe and cost effective. In traditional medicine several plants have been used as hepatoprotective but its efficacy and mode of molecular mechanism of drug action are seldom investigated. In the present investigation, 92 phytochemicals from three plant species viz., Allamanda cathartica L., Solanum indicum L. and Vigna mungo L., which have been used as hepatoprotective plants in Indian traditional systems of treatment, were docked with the HBc protein. The structures of phytochemicals were procured from open access databases or drawn using MarvinSketch and 3D structure of the target protein, HBc was downloaded from protein data bank (PDB ID: 1QGT). Docking was carried out in AutoDock 4.2 and the results indicated that all the three plants have anti-hepatitis B activity and among the three plants the most potential lead molecule; carpesterol was identified from Solanum indicum.*
Keywords: *AutoDock, Allamanda cathartica, Docking, Hepatitis B, Phytochemicals, Solanum indicum, Vigna mungo,*

I. Introduction

Liver, the metabolic engine is a vital organ involved in metabolic pathways of the body related to growth, development, immunity etc. It is a frequent target for a number of toxicants which may cause liver cirrhosis or hepatitis. The hepatitis B, a life-threatening liver infection is caused by hepatitis B virus. Around 240 million people are chronically infected with hepatitis B and more than 7,80,000 people die yearly [1]. Human hepatitis B virus (HBV), the prototype member of the family hepadnaviridae is a circular partially double-stranded DNA virus of approximately 3200 nucleotides. The highly compact genome contains the four major open reading frames (ORFs) encoding the envelope (Pre S1, Pre S2, and surface antigen HBsAg), core (Pre core precursor protein, HBeAg and HBcAg) polymerase (HBPol) and X (HBx) proteins respectively [2]. The infectious HBV virions (Dane particles) has a spherical, double-shelled structure of 42nm in diameter, consisting of a lipid envelope containing HBsAg that surrounds an inner nucleocapsid composed of core antigen (HBcAg) complexes with the virally encoded polymerase and the viral DNA genome [3].

The major goal of hepatitis B treatment is to prevent serious infections like cirrhosis, liver decompensation and hepatocellular carcinoma (HCC). In clinical practice, treatment response is determined by suppression of serum HBV DNA levels, hepatitis B e antigen (HBeAg) seroconversion to hepatitis B antibody, hepatitis B surface antigen (HBsAg) loss, normalization of alanine aminotransferase levels and improvement in liver histology. Clinical treatments involving nucleotide/nucleoside analogues and interferon have limited success due to drug resistance mutants [4].

Medicinal plants, the backbone of traditional medicine with excessive pharmacological studies are the potential source of lead compounds in drug development. Plants being rich sources of secondary metabolites such as alkaloids, flavanoids, terpenoids, triterpenies, tannins, phenolic compounds, etc. have been used as treatment option including liver ailments [5]. They have been evolved through biological validation and therefore induce less toxicity and side effects as compared to synthetic drugs. The present investigation aimed to validate the hepatoprotective activity and identification of lead molecules in three medicinal plants *viz., Allamanda cathartica* L., *Solanum indicum* L. and *Vigna mungo* L. through molecular docking. *Allamanda cathartica* L. is a tropical twining vine with deeply veined whorled leaves and bright yellow flowers. The phytochemical constituents include iridoid lactones and iridoid glycoside [5]. *Solanum indicum* L., belongs to the family Solanaceae with a bushy herb containing prickly spikes in the stem. The fruit is used as a common vegetable by South Indian people. Apart from glycosides, saponins, flavanoids, tannins and steroids were reported [6]. *Vigna mungo* L. is a member of Leguminosae with an erect to sub-erect, hairy, annual herb with long twining branches. It has been used in the Indian traditional systems of medicine for various ailments. The phytochemical constituents include saponins, alkaloids, volatile oils, flavanoids, and anthraquinones [7].

II. Materials and Methods

2.1 Preparation of receptor- Human hepatitis B viral capsid protein

The X-ray crystallographic structure of the receptor molecule, HBcAg was obtained from the Protein Data Bank (PDB ID: 1QGT). The active site residues were determined using CO-FACTOR, a structure-based method for biological function annotation of a protein molecule. It first identifies template proteins of similar folds and functional sites by threading the target structure through three representative template libraries that have known protein-ligand binding interactions, enzyme commission number or gene ontology terms [8]. Finally, it will provide a list of proteins having the structural similar binding site with the query protein. The active site residues were identified as PRO25, ASP29, LEU30, THR33, TRP102, SER106, PHE110 and VAL115.

2.2 Preparation of ligands - Phytochemicals

Based on traditional knowledge, literature survey and availability, three plant species*, viz., Allamanda cathrtica* L*., Solanum indicum* L. and *Vigna mungo* L. were selected. The phytochemical details reported from the foregoing plants were collected from chemical databases *viz.,* PubChem and ChemSpider and a molecular weight less than 900g/mol were selected for docking. The chemical structures of compounds unavailable in open access databases were modelled using MarvinSketch 15.3.30.0 and the 3D structures were generated in CORINA. A total of 92 phytochemicals were chosen, 27 from *Allamanda cathartica* L., 20 from *Solanum indicum* L. and 45 from *Vigna mungo* L.. The list of molecules used for docking is depicted in Table 1.

2.3 Molecular docking

Open access docking tool AutoDock version 4.2 was used to carry out docking of phytochemicals [9]. This tool uses Monte Carlo Simulated Annealing and Lamarckian genetic algorithm for the generation of possible orientations of ligand at the binding site of the target. Set the spacing between grid points to $0.425A^0$ and number of points in the X, Y and Z dimensions to 60, 60 and 60; so that the total grid points per map is to 226981. In order to centre the grid box on the active site of the target XYZ-coordinates were set to 111.526 A°, 74.575 A°, 50.963 A°. For docking, all the parameters were kept as default including population number. The ligand-bound complexes were analysed considering the lowest binding energies and interaction forces.

2.4 Prediction of drug likeness using molinspiration

Molinspiration uses sophisticated Bayesian statistics to compare structures of the representative ligands, active on the particular target site. It calculates the drug-likeness properties using LogP (octanol/water partition coefficient), molecular polar surface area (TPSA), molecular volume, the rule of five properties and the number of rotatable bonds [10].

2.5 Visualization of docked structure using Discovery Studio Visualizer

The Discovery Studio Visualizer is a free viewer that can be used to open data generated by other software in the Discovery Studio product line. It is designed to offer an interactive environment for viewing and editing molecular structures, sequences, X-ray reflection data, scripts and other data. It also provides a rich set of viewers for displaying plots and other graphical representations of data. For the present study, Discovery Studio Visualizer 4.5 was used to analyse the docked structures [11].

III. Results and Discussion

3.1 HBc as target protein

The 21kDa core protein did not show any structural analog in human. It regulates the essential functions including genome packaging, reverse transcriptase and intracellular trafficking [12]. The crystal structure of Hepatitis B virus core protein in $3.3A^0$ resolution showed a large helical protein fold which is unusual in icosahedral viruses. The monomer fold stabilized by a hydrophobic core which was highly conserved among human variants [13]. The 183/185 (depending upon genotype) residue protein consists of a 149 residue assembly domain and 34/36 residue RNA binding C-terminus domain. The first 149 residues form the α-helix rich assembly domain and the last 34/36 residues form the arginine rich C-terminus domain. The major role of the HBV capsid is to pack nucleic acids and shuttle them to nucleus. The C-terminus of the HBV core protein starting from amino acid residue proline144 and therefore, the entire 'Arg' rich region is dispensable for core assembly whereas truncations beyond amino acid 140 are not tolerated. The presence or absence of Arg rich tail does not markedly influences the electrophoretic mobility of particles. The assembly capability of the HBV core protein resides in its first 140 to 144 amino acids [14]. It is apparent that a conserved hydrophobic core is responsible for stabilization of the monomer fold, while residues 120-143 form crucial interactions that stabilise the structure of capsid. Phytochemicals that target the Hepatitis B virus core

protein assembly domain can disrupt the functional HBV capsid assembly and can be a potent inhibitor of HBV replication. Small molecules that target the HBV core protein assembly domain can disrupt the functional HBV capsid assembly and can be potent inhibitors of HBV replication [13].

3.2 Docking analysis

The ligand-bound complexes were analysed for its binding affinity and possible orientations were ranked according to lowest binding energy through cluster analysis. From the docking calculation, the conformer with minimum binding energy was picked from 10 runs/pose. In general, docked structures having a free energy of binding less than -5.0 kcal/mol has been considered as hit molecules. Out of 27 phytochemicals from *Allamanda cathartica* 19 of them showed binding energy $\leq$ -5.0 kcal/mol. Similarly, out of 20 molecules screened from *Solanum indicum* 16 of them and out of 45 molecules from *Vigna mungo* 29 of them showed binding energy $\leq$ -5.0 kcal/mol. Therefore, molecules having binding energy $\leq$ –7 kcal/mol were selected as hits. The details of docked results of hit molecules were depicted in Table 2. The selected hit molecules were ursolic acid (ΔG_{bind} -8.82), squalene (ΔG_{bind} -7.96) and allamandicin (ΔG_{bind} -7.25) from *Allamanda cathartica,* carpesterol (ΔG_{bind} -10.65), solasodine (ΔG_{bind} -10.55) and solamargine (ΔG_{bind} -9.42) from *Solanum indicum* and cyclokievitone (ΔG_{bind} -9.11), 4'-o-methylkievitone (ΔG_{bind} -8.0) and 2',4',7-trihydroxyisoflavaone (ΔG_{bind} -7.88) from *Vigna mungo* respectively.

3.3 Visualizations using Discovery Studio Visualizer

The docked structures of hit molecules with the target protein were observed in Discovery Studio Visualizer and the details of bonds and interactions were recorded. The hit molecules from *Allamanda cathartica viz.* allamandicin, ursolic acid and squalene showed no hydrogen bonds. Similarly, among the three selected hits from *Solanum indicum* the compound solasodine showed no hydrogen bond interaction with the core protein but it had least free energy of binding (ΔG_{bind} -10.53 kcal/mol). Maximum numbers of hydrogen bond interactions (4 nos) were observed with solamargine but only two hydrogen bonds were observed with the active site residues ASP29 and TRP102 respectively. The third molecule, carpesterol showed the least free energy of binding and 2 hydrogen bonds with the active site residues, TRP102 and SER106 (Fig. 1a & b). The known inhibitor AT-130, a phenylpropenamide derivative was bound to the hydrophobic core pocket in HBV capsid formed by TRY118, TRP102 and PRO25 and formed multiple connections with the binding site and it blocks the HBV replication at the level of viral RNA packaging [15]. Among the hit molecules from *Vigna mungo,* cyclokievitone (ΔG_{bind} -9.11 kcal/mol) showed a sulphur hydrogen bond and a hydrogen bond with bond distance 2.74 A^0 and 2.66 A^0 respectively (Fig. 1c). 4'-o- methylkievitone (ΔG_{bind} -8.00kcal/mol) showed a single hydrogen bond with CYS107 (2.99 A^0) which is one among the 4 cysteine residues (CYS48, CYS61, CYS107and CYS183) (Fig. 1d). 2', 4', 7-trihydroxyisoflavaone showed three hydrogen bond interactions with ΔG_{bind} -7.88 kcal/mol (Fig. 1e). It fits into a well-defined, largely hydrophobic pocket created by PRO25 (2.69 A^0), SER26 (3.00 A^0) and LEU31 (3.14 A^0).

The molecular properties of all possible hits were calculated by molinspiration (Table 3). The compounds allamandicin, cyclokievitone, 4'-o-methylkievitone and 2',4',7-trihydroxyisoflavaone showed no violation; ursolic acid, solasodine and squalene showed 1 violation each; and carpesterol and solamargine showed 2 and 3 violations respectively. In general, drug molecules evolved out of natural compounds violate Lipinski's rule of five [16]. For instance, all-time best selling prescription drug for cholesterol lowering, Lipitor (Pfizer's trade mark for atorvastatin), violate two of the Lipinski's rules (mol wt. and clogp) [17]. Among the hit molecules obtained from three plants the compound, carpesterol from *Solanum indicum* showed lowest free energy of binding, two H-bonds with active residues and also showed hydrophobic alkyl and pi-alkyl bonds at the hydrophobic core of LEU119, LEU140, LEU19, PRO25, PHE103, TYR118, PHE23 and PHE24 (Fig. 1b). Therefore, carpesterol was proposed as the best lead molecule.

IV.   Conclusion

The foregoing results demonstrated that all the three plants contain chemical molecules with anti-hepatitis B activity. Among them, the compound carpesterol derived from *Solanum indicum* can be considered as the best lead and therefore the same plant can be considered as the best hepatoprotective plant. However, *in vivo* and *in vitro* validation of the hit molecules is inevitable.

References

[1].   WHO report, July 2015 http://www.who.int/mediacentre/factsheets/fs204/en/
[2].   L. Stuyver, Sija De Gendt, C. V. Geyt, F. Zoulim, M. F., Raymond, F. Schinazi, and R. Rossau, A new genotype of hepatitis B virus: Complete genome and phylogenetic relatedness, *Journal of General Virology, 81,* 2000, 67-74.
[3].   T. J. Liang, Hepatitis B: The virus and disease, *Hepatology, 49(5),* 2009, S13-S21.
[4].   M. Arooj, M. Sattar, M. Safdar, S. Kalsoom, and S Shahzad, *In silico* molecular docking and design of anti-hepatitis B drugs, *IOSR Journal of Pharmacy and Biological Sciences, 3(6),* 2012, 41-55.
[5].   V. Prabhadevi, S. S. Sathish, M. Johnson, B. Venkatramani, and N Janakiraman, Phytochemical studies on *Allamanda cathartica* L. using GC-MS, *Asian Pacific Journal of Tropical Biomedicine, 1,* 2012, S550-S554.
[6].   B. Bhuvaneswar, M. Manimegalai, and L. Suguna, Hepatoprotective and antioxidant activities of *Solanum indicum* Linn. Beries, *International Journal of Clinical Toxicology, 2,* 2014, 71-76.
[7].   P. F Sherlina, V. Gayathri, and S. R. Radha, Preliminary phytochemical analysis of black gram, *Vigna mungo* L., *International Journal of Development Research, 3(11)*, 2013, 147-149.
[8].   Ambrish Roy, J. Yang, and Y. Zhang, COFACTOR: An accurate comparative algorithm for structure-based protein function annotation, *Nucleic Acid Research, 40*, 2012, W471-W477.
[9].   G. M. Morris, R. Huey, W. Lindstorm, M. F. Sanner, R. K. Belew, D. S. Goodsell, and A. J. Olson, AutoDock4 and AutodockTools4: Automated docking with selective Receptor flexibility, *Journal of Computational Chemistry, 30(16)*, 2009, 2785-2791.
[10]. P. Ertl, B. Rohde, and P. Selzer, Fast calculation of molecular polar surface area as a sum of fragment-based contributions and its application to the prediction of drug transport properties, *Journal of Medicinal Chemistry, 43(1),* 2000, 3714-3717.
[11]. Dassault Systems BIOVIA, Discovery Studio Modeling Environment, Release 4.5, San Diego: Dassault Systems, 2015.
[12]. C. Bourne, S. Lee, B. Venkataiah, A. Lee, B. Korba, M. G. Finn, and A. Zlotnick, Small-molecule effectors of hepatitis B virus capsid assembly give insight into virus life cycle, *Journal of Virology, 82(20),* 2008, 10262-10270.
[13]. S. A. Wynne, R. A. Crowther, and A. G. W. Leslie, The crystal structure of the human hepatitis B virus capsid, *Molecular Cell, 3*, 1999, 771-780.
[14]. F. Birnbaum, and M. Nassal, Hepatitis B virus nucleocapsid assembly: Primary structure requirements in the core protein, *Journal of Virology, 67(7),* 1990, 3319-3330.
[15]. Na Liu, F. Zhao, Haiyong Jia, Diwakar Rai, P. Zhan, X. Jiang, and X. Liu, Non-nucleoside anti-HBV agents: Advances in structural optimization and mechanism of action investigations, *Medicinal Chemistry Communication, 6(1),* 2015, 521-535.
[16]. N. C. Nisha, S. Sreekumar, C. K. Biju, P. N. Krishnan, Identification of lead compounds with cobra venom neutralising activity in three Indian medicinal plants, *International Journal of Pharmacy and Pharmaceutical Sciences, 6(2)*, 2014, 536-541.
[17]. M. Araujo de Brito, Pharmacokinetic study with computational tools in the medicinal chemistry course, *Brazilian Journal of Pharmaceutical Sciences, 47(4),* 2011, 797-805.

Table 1: List of phytochemicals used for docking

	Compound (Molecular formula, molecular weight (g/mol)		
		47.	Solavetivone ($C_{15}H_{22}O$), 218.34
	Allamanda cathartica		*Vigna mungo*
1.	1-deoxy-d-mannitol ($C_6H_{14}O_5$), 166.17		
2.	3, 7, 11, 15-tetramethyl-2-hexadecen-1-ol ($C_{20}H_{40}O$), 296.53	48.	2',4',7-trihydroxyisoflavone ($C_{15}H_{10}O_5$), 270.24
3.	3-o-methyl-d-glucose ($C_7H_{14}O_6$), 194.18	49.	2'-hydroxygenistein ($C_{15}H_{10}O_6$), 286.23
4.	6,7- dimethylthieno(2,3-b) quinolin-3-ylamine ($C_{13}H_{12}O_2$), 228.31	50.	4'-o-methylkievitone ($C_{45}H_{73}NO_{15}$), 868.07
5.	9,12-octadecadienoic acid, ethyl ester ($C_{20}H_{37}N_2S$), 309.51	51.	Allantoin ($C_4H_6N_4O_3$), 158.17
6.	Allamandicin ($C_{15}H_{17}O_7$), 309.29	52.	Ascorbic acid ($C_6H_8O_6$), 176.12
	Allamcin ($C_{13}H_{14}O_5$), 250.25	53.	Aureol ($C_{21}H_{30}O_2$), 314.46
8.	Beta-l-arabinopyranoside, methyl ($C_6H_{12}O_5$), 164.15	54.	Behenic acid ($C_4H_6N_4O_3$), 158.17
9.	Cis,cis,cis-7,10,13-hexadecatrienal ($C_{16}H_{26}O$), 234.38	55.	Benzeneacetamide (C_8H_9NO), 135.16
10.	Decanoic acid ($C_{16}H_{26}O$), 234.38	56.	Cellobiose ($C_4H_6N_4O_3$), 158.17
11.	Dodecanoic acid ($C_{12}H_{25}O_2$), 201.33	57.	Choline ($C_5H_{14}NO$), 104.17
12.	Ethyl A-d-glucopyranoside ($C_8H_{16}O_6$), 208.21	58.	Chrysanthemin ($C_4H_6N_4O_3$), 158.17
13.	Hexadecanoic acid, ethyl ester ($C_{12}H_{25}O_2$), 201.33	59.	Coniferin ($C_{16}H_{22}O_8$), 342.34
14.	Hexadecanoic acid ($C_{16}H_{33}O_2$), 257.43	60.	Cyclokievitone ($C_{20}H_{18}O_6$), 354.35
15.	Hexanoic acid ($C_8H_{17}O_2$), 145.22	61.	Dalbergionidin ($C_{15}H_{12}O_6$), 288.25
16.	Isoplumericin ($C_{15}H_{15}O_6$), 291.27	62.	Dehydroascorbic acid ($C_6H_6O_6$), 174.10
17.	Nonadecanoic acid, ethyl ester ($C_{16}H_{33}O_2$), 257.43	63.	Diethylstilbestrol ($C_4H_6N_4O_3$), 158.17
18.	Octadecanoic acid, ethyl ester ($C_{20}H_{41}O_2$), 313.54	64.	Folic acid ($C_{19}H_{21}N_7O_6$), 443.42
19.	Octanoic acid ($C_{10}H_{21}O_2$), 173.27	65.	Genistein ($C_{15}H_{10}O_5$), 270.24
20.	Oleic acid ($C_{18}H_{35}O_2$), 283.47	66.	Glutathione ($C_{10}H_{19}N_3O_6S$), 309.34
21.	Pentadecanoic acid ($C_{15}H_{31}O_2$), 243.41	67.	Glycinol ($C_{15}H_{12}O_5$), 272.25
22.	Plumericin ($C_{15}H_{15}O_6$), 291.27	68.	Hydroxygenistein ($C_{15}H_{12}O_5$), 272.25
23.	Plumieride coumarate glucoside* ($C_{30}H_{33}O_{14}$), 617.58	69.	Hydroxylamine (H_3NO), 33.03
24.	Plumieride ($C_{16}H_{33}O_2$), 257.43	70.	Indole-3-acetamide ($C_{10}H_{10}N_2O$), 174.20
25.	Squalene ($C_{30}H_{50}$), 410.73	71.	Isovitexin ($C_{10}H_{19}N_3O_6S$), 309.34
26.	Tetradecanoic acid ($C_{16}H_{33}O_2$), 257.43	72.	Lignoceric acid ($C_{24}H_{49}O_2$), 369.65
27.	Ursolic acid ($C_{30}H_{49}O_3$), 457.71	73.	Linoleic acid ($C_{18}H_{33}O_2$), 281.46
	Solanum indicum	74.	Linolenic acid ($C_{18}H_{31}O_2$), 279.44
28.	Beta-sitosterol glucoside ($C_{35}H_{60}O_6$), 576.85	75.	Melibiose ($C_{12}H_{22}O_{11}$), 342.29

29.	Beta-sitosterol ($C_{29}H_{50}O$), 414.71	76.	Nicotiflorin ($C_{27}H_{30}O_{15}$), 594.52
30.	Caffeic acid ($C_{16}H_{33}O_2$), 257.43	77.	Oleic acid ($C_{18}H_{35}O_2$), 283.47
31.	Caffeoylquinic acid ($C_{34}H_{37}O_{15}$), 685.655	78.	Oxalic acid ($C_2H_4O_4$), 92.05
32.	Carotene ($C_{40}H_{72}$), 553.01	79.	Palmitic acid ($C_{16}H_{33}O_2$), 257.43
33.	Carpesterol ($C_{37}H_{54}O_4$), 562.83	80.	P-hydroxycinnamic acid ($C_9H_{11}O_3$), 167.18
34.	Dioscin ($C_{45}H_{72}O_{16}$), 869.05	81.	Raffinose ($C_{18}H_{32}O_{16}$), 504.43
35.	Diosgenin ($C_{27}H_{42}O_3$), 414.63	82.	Riboflavin ($C_{17}H_{20}N_4O_6$), 376.36
36.	Indioside E* ($C_{44}H_{70}O_{16}$), 855.02	83.	Robinin ($C_{33}H_{40}O_{19}$), 740.66
37.	Lanosterol ($C_{27}H_{42}O_3$), 414.63	84.	Shikimic acid ($C_7H_{11}O_5$), 175.16
38.	Methyl protodioscin ($C_{52}H_{86}O_{22}$), 1063.23	85.	Soyasaponin I* ($C_{48}H_{79}O_{18}$), 944.14
39.	Naringenin ($C_{15}H_{12}O_5$), 272.25	86.	Soyasaponin II* ($C_{47}H_{77}O_{17}$), 914.11
40.	p-coumaric acid ($C_9H_{11}O_3$), 167.18	87.	Soyasaponin III* ($C_{42}H_{69}O_{14}$), 798.00
41.	Protodioscin ($C_{51}H_{84}O_{22}$), 1049.21	88.	Stachyose ($C_{24}H_{42}O_{21}$), 666.57
42.	Scopoletin ($C_{10}H_8O_4$), 192.17	89.	Stearic acid ($C_{18}H_{37}O_2$), 285.49
43.	Solafuranone* ($C_{15}H_{20}O_2$), 232.32	90.	Urea (CH_4N_2O), 60.05
44.	Solamargine ($C_{45}H_{73}NO_{15}$), 868.07	91.	Verbascose ($C_{30}H_{52}O_{26}$), 828.72
45.	Solasodine ($C_{27}H_{43}NO_2$), 413.64	92.	Vitexin ($C_{21}H_{20}O_{10}$), 432.38
46.	Solasonine ($C_{45}H_{73}NO_{15}$), 868.07		

* drawn using MarvinSketch 15.3.30.0

Table 2: Selected hit molecules from three plants against HBcAg in AutoDock4

Plant	Phytochemicals	ΔG bind (kcal/mol)	kI	Mol wt(g/mol)	Ligand Efficiency	Run
A. cathartica	Ursolic acid	-8.82	340.0nM	456.70032	-0.27	1
	Allamandicin	-7.25	4.81uM	308.28334	-0.33	9
	Squalene	-7.96	1.47uM	410.718	-0.27	6
S. indicum	Carpesterol	-10.65	15.63nM	562.84	-0.26	8
	Solamargine	-9.42	124.79nM	868.05882	-0.15	4
	Solasodine	-10.53	18.60nM	413.63582	-0.34	10
V.mungo	Cyclokievitone	-9.11	211.0nM	354.35332	-0.35	6
	4'-o-Methylkievitone	-8.0	1.37uM	370.39578	-0.30	4
	2',4',7-trihydroxyisoflavaone	-7.88	1.68uM	270.2369	-0.39	5

Table 3: Drug likeness properties of hit molecules in molinspiration

Lead molecule	Mol wt (g/mol)	miLogP	H-bond donor	H-bond acceptor	Violations
Ursolic acid	456.70032	7.3	2	3	1
Allamandicin	308.28334	0.5	1	7	0
Squalene	410.718	11.6	0	0	1
Carpesterol	562.84	9.01	1	4	2
Solamargine	868.05882	1.1	9	16	3
Solasodine	413.63582	5.4	2	3	1
Cyclokievitone	354.35332	3.5	3	6	0
4'-o-Methylkievitone	370.39578	4.5	3	6	0
2',4',7-trihydroxy isoflavaone	270.2369	2.1	3	5	0

Table 4: List of hit molecules with bond type, bond length, binding residues

| Lead molecules	Bond Type	Bond details	Bond Length (A^0)	Binding Residues
Ursolic acid	No H bond			
Allamandicin	No H bond			
Squalene	No H bond			
Carpesterol	O-H…O	UNK1:H88…TRP102:O	1.98	TRP102
	C-H…O	SER 106:C…UNK1:O38	2.82	SER106
Solamargine	O-H…O	UNK1:H…ASP29:O	1.94	ASP29
	O-H…O	UNK1:H…PHE23:O	2.08	PHE23
	O-H…O	UNK1:H… PHE23:O	1.84	PHE23
	O-H…O	UNK1:H…TRP102:O	2.21	TRP102
Solasodine	No H bond			
Cyclokievitone	O-H…O	UNK1:H41…VAL115:O	2.74	VAL115
	S-H…O	UNK1:H40…CYS107:SG	2.66	CYS107
4'-o-Methylkievitone	S-H…O	CYS107:SG…UNK1:O22	2.99	CYS107
2',4',7-trihydroxy isoflavaone	O-H…O	UNK1:H25…PRO25:O	2.69	PRO25
	O-H…O	UNK1:H24…SER26:O	3.00	SER26
	N-H…O	LEU31:N…UNK1:O7	3.14	LEU31
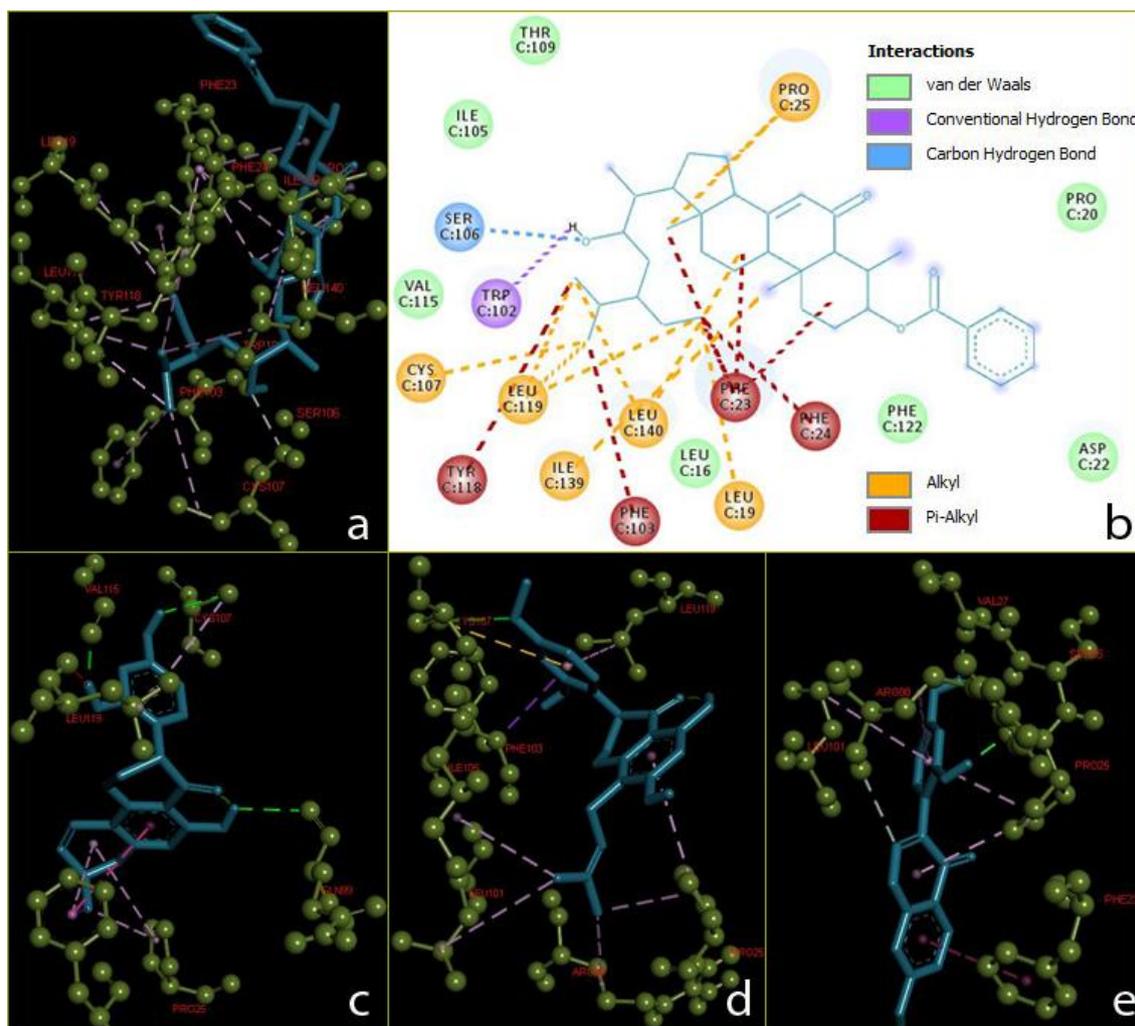
Figure 1. Docking interaction: a & b. HBc protein and carpesterol, c. HBc and cyclokievitone, d. HBc and 4'-o-methylkievitone, e. HBc and 2',4',7'- trihydroxyisoflavanone